Available online at www.sciencedirect.com
ScienceDirect
Journal of Sound and Vibration 312 (2008) 769–788
JOURNAL OF SOUND AND VIBRATION
www.elsevier.com/locate/jsvi

Free vibration of advanced anisotropic multilayered composites with arbitrary boundary conditions

Roland L. Woodcock*

United Technologies Research Center, Acoustics Group, Components Department, 411 Silver Lane, MS 129-17, East Hartford, CT 06108, USA

Received 4 May 2006; received in revised form 14 October 2007; accepted 7 November 2007
Available online 2 January 2008

Abstract

Advanced composite stratified structures are of particular interest in numerous industrial areas such as the aerospace and aircraft industries. The main feature of these anisotropic materials is their ability to be tailored for specific applications by optimizing design parameters such as stacking sequence, ply orientation and performance targets. Designing through optimization principles requires the knowledge of an objective function which integrates all the unknowns of the materials therefore an accurate component-level modeling of stratified structures is necessary. Classical formulation available in the literature typically assumes a number of unknowns that increases with the number of layers and this sets serious limitations when trying to solve practical problems. As an alternative an advanced generalized modeling of multilayered composites with arbitrary boundary conditions is proposed in the present paper. This formulation is of a hybrid type which combines the advantages of both single-layer of the First Shear Deformation Theory and multi-layered approach. The number of unknowns is completely independent of the number of layers and a rigorous transfer matrix approach is developed from the interface conditions, which allows the parameters of the last layer to be iteratively related to those of the first layer. The Rayleigh–Ritz method is used in conjunction with a non-orthogonal polynomial basis to establish the free vibration. The model is then validated under free–free boundary conditions against data available in the literature in the case of isotropic, anisotropic angle-ply composites. Excellent agreement is obtained with a relative error less than 1%, which assesses the validity of the present model. In addition a sensitivity analysis is performed on the boundary stiffness required to model boundary conditions to illustrate the complexity associated with the arbitrary boundary conditions when using artificial springs.

1. Introduction

In this paper the modeling of advanced multi-layered composites is addressed. These types of models are being used increasingly in aerospace and aircraft applications. A great number of papers have been published with emphasis for review articles for a state of the art, especially regarding free vibration modeling. It is out of the scope of this paper to attempt to give an exhaustive review on this topic. The reader is referred for example

*Corresponding author at: Hawker Beechcraft Corporation, Acoustics Group, 9709 E. Central, Wichita, KS 67206, USA. Tel.: +1 316 676 7391.
E-mail address: roland_woodcock@hawkerbeechcraft.com

0022-460X/$ - see front matter © 2007 Elsevier Ltd. All rights reserved.
doi:10.1016/j.jsv.2007.11.015

to Ref. [1] concerned with a fairly comprehensive overview of the subject. From a structural point of view, the methods used to model composite multi-layers can be split into three main categories: (1) an approach of single-layer type, (2) a "pure" multi-layer modeling, (3) a multi-layer formulation of hybrid type.

1.1. Approach of single-layer type

The approach of single-layer type consists in replacing the multi-layer by one homogeneous layer with equivalent mechanical properties which are calculated for example by the classical mixture law [2]. In this category two types of models are of interest: (i) "Classical Laminate Theories" [3] based on thin plate theories of Love–Kirchoff, which assume that the orthogonality of lines with respect to the neutral axis is kept during the deformation. The thickness of the composite is assumed to be small compared to the wavelength. (ii) Those based on Mindlin's thick plate theories and referenced as "Shear Deformation Theories", which are more rigourous with increasing frequency. These approaches are characterized by the account of a shear effect, which means that the orthogonality properties previously mentioned are no longer valid. The shear deformation theories have led to many categories with different levels of sophistication. Two main levels are commonly employed. First, the high-order shear deformation theories include powers of higher orders in the displacement field such as the first-order model (i.e. first-order shear deformation theory [4]). Second, the generalized shear deformation theory [5]; this model includes as special cases the models previously mentioned. It has been established in the literature that classical laminate theories tend to overpredict the natural frequencies.

1.2. Multi-layer approach

A multi-layer is characterized by the type of interface between two layers. Two types of interface are generally encountered: (i) interfaces of rigid type, (ii) and those of non-rigid one. The multi-layers of the first type characterize the structures for which a relationship between the parameters of the different layers exists. For example it is assumed that the transverse displacement is kept identical for all the layers. This is the case of sandwich structures, which include as an example honeycomb layers. This assumption does not stand for multi-layers of the second type for which sandwich structure with a flexible core is an example. These layers support classical waves (bending, membrane and shear) and also a dilatational mode due to a deformation in the thickness direction, which is a consequence of a low shear modulus. Multi-layers of the first type have been studied in the literature from a structural point of view. The proposed models have two advantages: (i) they explicitely include the phenomena present in each layer; (ii) they adequately describe interface conditions. This is the case of the interlaminar shear stress continuity theory [6], which is based on the continuity of the displacements and of the shear stress at the interface and which satisfies free shear traction conditions on the laminate surfaces. The disadvantage of this modeling is that the number of unknowns increases with the number of layers. This limitation has led researchers to study only multi-layers with very few layers [7].

Multi-layers of the second type have been studied either in the general case [6], or in the case of three-layered structures [8–10] generally with a certain number of assumptions: the faces support bending waves (eventually + in-plane motions) and the core is assumed to support one more wave: shear effect.

With regard to boundary conditions, only simply supported and clamped conditions are the most boundary conditions reported in the literature. In Ref. [11] a finite three-layer model was presented with mixed boundary conditions in the sense that two opposite sides were simply supported while two others were of an elastic type.

1.3. Multi-layers of hybrid type

The last category deals with multi-layers of hybrid type [7,13,14], which combines the advantages of the two preceding approaches: the displacement field is defined in each layer and appropriate interface conditions are used between two adjacent layers. The technique described in Ref. [14] combines the advantages of the interlaminar shear stress continuity theory and the high-order shear deformation theory previously described. This hybrid approach allows the multi-layers to be reduced to a four-layer system using some appropriate interface conditions. In Ref. [7] a model, which accounts for local rotations including both flexural and shear

effects was proposed. The principle exposed in that paper showed that it is possible to express the different energies in terms of the parameters of the first layer. The approach used in Refs. [12,13] follows the same philosophy and is very interesting since it allows the multi-layer to be replaced by a single layer while keeping the description of the whole system. Appropriate transfer matrices were defined from interface conditions, which allow the parameters of the last layer to be related to those of the first one. All the vibro-acoustic indicators are calculated from the unknowns of the first layer. However (i) the boundary conditions are restricted to simply supported, (ii) the laminae are modeled as specially orthotropic layers. This approach allows only multi-layers of the first type (rigid interface) to be simulated. But this is not a severe limitation since it remains possible to cover a great number of structures encountered in practice, in particular in aircraft and aerospace areas. There is a second element in favor of this approach: multi-layers of the second type (non-rigid interface) can exhibit dilatational modes and for typical structures these effects appear in the high-frequency range; this is not a limitation since the effect of the boundary condition is suspected to be important in the low-frequency range [15]. The advantage of this approach is that it offers a great flexibility regarding the number of layers. The number of unknowns does not increase with the number of layers.

1.4. The present work

The present work takes advantage of the hybrid-type formulation for dealing with the multi-layers. Typically layerwise models are based on avoiding violating physical continuities at the interface between layers. The present paper is concerned with a general modeling of multi-layered structures with different aspects of generalization [17], which enhance the approach proposed in Ref. [12] in order to extend the application to more complicated advanced composite materials. (i) Each layer supports the classical waves present in a solid medium: bending, membrane, shear and rotatory inertia effects; (ii) the generalization of the orthotropic properties to the case of anisotropic layers is included by means of a general orthotropy in the Oxy plane as adopted in Ref. [16]; (iii) a general modeling of arbitrary boundary condition of elastic type is done by means of artificial springs acting on each effect of the first layer (since it is the equivalent system). Such boundary condition modeling allows the simulation of real conditions, which lie between classical extreme cases namely simply supported and clamped conditions. Although the boundary condition modeling is outlined in the present paper in its general description, the paper will focus on free–free boundary condition in order to fully validate the structure operator as a first step.

The displacement field adopted to describe point (i) has been proposed in Refs. [7,12,13]. Point (ii) is the generalization to the case of anisotropic composites as most of plies encountered in the industry exhibit this property. And (iii) is the generalization of the formulation developed for a generally orthotropic single-layer composite as shown by Woodcock and Nicolas [16]. It will now be possible to investigate soft boundary condition, which practice has shown to be attractive, for example when using viscoelastic materials for sealings. It must be noticed that when dealing with an anisotropic single layer with an orthotropy angle with respect to the natural axes of the plate different of zero to simulate fiber orientations in an unidirectional composite, the present formulation should be preferred to the model presented in Ref. [16] as the proposed displacement field in the present paper is more accurate since it accounts for the in-plane waves as well (stretching and shearing).

The methods used to deal with the free vibration of composite plates can be split roughly in two main categories: (1) analytical methods such as classical modal analysis (CMA) [12] or the method of superposition [29]; (2) approximate methods such as finite element analysis or expansion-type of techniques, i.e. Rayleigh–Ritz and Galerkin methods. Finite element analysis is appropriate to deal with systems with complex shape and geometry. The Rayleigh–Ritz method is well suited to model arbitrary boundary conditions. The success of Rayleigh–Ritz methods relies on the proper choice of admissible functions for the basis [28]. Typical functions include orthogonal polynomials [30], simple polynomials [31] or beam functions. Many research papers have been published on the Rayleigh–Ritz methods. It is out of the scope of the present paper to attempt to list the relevant articles on the subject. The reader can consult for example Refs. [32,33] for an interesting discussion of the method. It must be kept in mind that typically when used to model multi-layers Rayleigh–Ritz methods deal with global displacement field, which makes it dependent on both the number of terms in the series and the number of layers.

In the present paper the governing differential equations of motion are derived using the Rayleigh–Ritz method. Each of the unknowns (bending, membrane, shear) is expanded on a non-orthogonal polynomial basis. This basis is retained in order to deal with arbitrary boundary conditions. The action of the different springs is critical; the boundary condition derived from minimizing the function of Hamilton in the case of simple support provides guidance to help positioning the different springs.

2. Theoretical analysis

2.1. Statement of the problem

Fig. 1 shows the baffled multi-layer made of N layers of dimensions a and b in the x and y direction, respectively. Each layer has a thickness denoted as h_n. The layers are numbered from 1 to N starting from the upper layer with the origin of the system located at the center of the mid-system. Each layer is modeled as a general orthotropic structure in order to account for anisotropic properties in a context of a bi-dimensional modeling. The general orthotropy is therefore described by means of two axes OX and OY, which make an angle θ_o with respect to the natural axes of the layers. The coordinates in the Cartesian system will be denoted (x, y, z). The general philosophy is to derive the governing differential equations for free vibration using the variational method. This consists in first expressing an energy function in terms of kinetic and deformation energies and then minimizing this function using the classical Rayleigh–Ritz method, which in this case requires each of the unknowns to be expanded on a functional basis. Minimizing the function of Hamilton leads to the governing differential classical equation of the form:

$$\mathscr{O}_p\{\mathscr{A}_{nm}\} = \{0\}, \tag{1}$$

where $\mathscr{O}_p$ is an operator of the multi-layer which is a function of mass and stiffness properties, $\{\mathscr{A}_{nm}\}$ is the vector of the coefficients of the different parameters in the basis. In the following, these different quantities will be established.

2.2. Theoretical model of the multi-layer

The displacement field adopted in the present modeling follows the model proposed in previous work [7,12]. In their modeling, the multi-layer was replaced by an equivalent layer. The principle consists in iteratively relating the parameters of the last layer to those of the first layer by using appropriate interface conditions to define transfer matrices; the unknowns are therefore those of the first layer. The description of each layer is based on the shear deformation theory assumptions: (i) the displacement gradients are small, i.e. linear

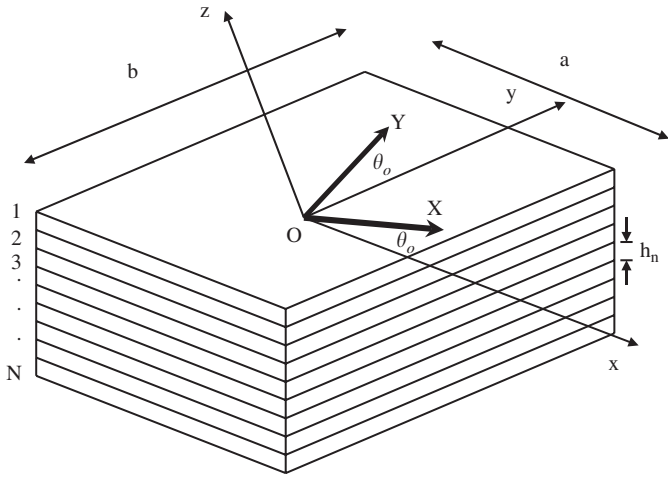

Fig. 1. Sketch illustrating the baffled multi-layered structure.

hypothetis; (ii) the in-plane motions are accounted for; (iii) the lines orthogonality with respect to the neutral axis is not conserved during the deformation: this corresponds to an account of a shear effect according to Mindlin's theory.

The modeling of the multi-layer in the present paper is based on the following assumptions: (i) the displacement field (U, V, W) is defined for each layer; (ii) the transverse displacement is kept identical for each layer which means that all the layers are rigidly bonded; (iii) the interface conditions are concerned with two conditions: the equality of the displacements and of the shear stresses; (iv) a general orthotropy is included in each layer.

The displacement field of each layer is written as follows [12]:

$$U^n(x,y,z) = \phi_x^n(x,y) + (R_n - z)\left(\frac{\partial W}{\partial x}(x,y) + \varphi_x^n(x,y)\right),$$

$$V^n(x,y,z) = \phi_y^n(x,y) + (R_n - z)\left(\frac{\partial W}{\partial y}(x,y) + \varphi_y^n(x,y)\right),$$

$$W^n(x,y) = W, \tag{2}$$

where W, ϕ_x^n, ϕ_y^n, φ_x^n, φ_y^n are the transverse displacement, the membrane along x and y direction, and the shear along x and y direction, respectively; R_n is an arbitrary coordinate due to the fact that a neutral axis cannot be defined. This displacement field contains as special case Love–Kirchoff's model for which only the term $\partial W(x,y)/\partial s$ is retained, s being x or y. The general field shows that each component contains the in-plane motion in addition to a rotation. This rotation is due to two contributions: the classical bending effect and shear effects.

The strain field ε_{ij} is given by

$$\varepsilon_{ij} = \frac{1}{2}\left(\frac{\partial U_i}{\partial x_j} + \frac{\partial U_j}{\partial x_i}\right). \tag{3}$$

It is assumed that U_1, U_2, U_3 stand for U, V, and W, respectively, and x_1, x_2 and x_3 stand for x, y, and z, respectively. In the context of a general modeling for the orthotropic properties, the stresses σ_{ij} and the deformations are related by the following matrix relations:

$$\begin{pmatrix} \sigma_{xx}^n \\ \sigma_{yy}^n \\ \sigma_{xy}^n \\ \sigma_{yz}^n \\ \sigma_{xz}^n \end{pmatrix} = \begin{pmatrix} Q_{11}^n & Q_{12}^n & Q_{16}^n & 0 & 0 \\ Q_{12}^n & Q_{22}^n & Q_{26}^n & 0 & 0 \\ Q_{16}^n & Q_{26}^n & Q_{66}^n & 0 & 0 \\ 0 & 0 & 0 & Q_{44}^n & Q_{45}^n \\ 0 & 0 & 0 & Q_{45}^n & Q_{55}^n \end{pmatrix} \begin{pmatrix} \varepsilon_{xx}^n \\ \varepsilon_{yy}^n \\ 2\varepsilon_{xy}^n \\ 2\varepsilon_{yz}^n \\ 2\varepsilon_{xz}^n \end{pmatrix}, \tag{4}$$

The first sub-matrix expresses the relations in the Oxy plane. This sub-matrix is full in order to account for the general orthotropy by means of the terms Q_{16} and Q_{26}. The present model contains as special case the orthotropic model proposed in Ref. [13] in which the orthotropic axes were aligned with the geometrical axes of the structure. Their model are retrieved by setting $Q_{16} = Q_{26} = 0$ and $Q_{44} = Q_{55} = Q_{66}$. Their modeling resulted in a diagonal submatrix in the Oyz and Oxz as a consequence of restricting the layers to be isotropic. The Q_{ij} also account for the angle of orthotropy and are related to the global parameters by a rotation matrix (see for example Eq. (8) in Ref. [16]). The Q_{ij} are calculated from the macroscopic engineering parameters:

$$\overline{Q_{11}} = \frac{E_x}{1 - \nu_x\nu_x}; \quad \overline{Q_{12}} = \frac{\nu_1 E_y}{1 - \nu_x\nu_y} = \frac{\nu_y E_x}{1 - \nu_x\nu_y}; \quad \overline{Q_{22}} = \frac{E_y}{1 - \nu_x\nu_y}; \quad \overline{Q_{66}} = G_{xy}; \tag{5}$$

$$\overline{Q_{44}} = G_{yz}; \quad \overline{Q_{55}} = G_{xz}, \tag{6}$$

where E_x, E_y, ν_x, ν_y and G_{xy} are the five parameters which fully characterize the plate in the Oxy plane. They are the Young's modulus in x and y directions, the Poisson ratio in x and y directions and the shear modulus. G_{xz} and G_{yz} are the shear modulus in the two perpendicular other planes.

2.3. Interface conditions and transfer matrix

Interface conditions are necessary to help replace the multi-layers by a single equivalent layer. These conditions, which are of common use in multi-layer modeling, are the continuity of the displacements (U and V) and of the shear stresses (σ_{xz} and σ_{yz}). These two conditions were already used in Ref. [7] and are reported hereafter for convenience with other notations.

The conditions on the displacements are written as

$$-\frac{h_n}{2}\left(\frac{\partial W}{\partial x}+\varphi_x^n\right)+\phi_x^n=\frac{h_{n+1}}{2}\left(\frac{\partial W}{\partial x}+\varphi_x^{n+1}\right)+\phi_x^{n+1}, \tag{7}$$

$$-\frac{h_n}{2}\left(\frac{\partial W}{\partial y}+\varphi_y^n\right)+\phi_y^n=\frac{h_{n+1}}{2}\left(\frac{\partial W}{\partial y}+\varphi_y^{n+1}\right)+\phi_y^{n+1}, \tag{8}$$

The two following equations express the conditions on the shear stresses:

$$Q_{44}^n 2\varepsilon_{yz}^n+Q_{45}^n 2\varepsilon_{xz}^n=Q_{44}^{n+1}2\varepsilon_{yz}^{n+1}+Q_{45}^{n+1}2\varepsilon_{xz}^{n+1}, \tag{9}$$

$$Q_{45}^n 2\varepsilon_{yz}^n+Q_{55}^n 2\varepsilon_{xz}^n=Q_{45}^{n+1}2\varepsilon_{yz}^{n+1}+Q_{55}^{n+1}2\varepsilon_{xz}^{n+1}. \tag{10}$$

The preceding equations allow derivation of a transfer matrix. Following Ref. [12] the unknowns of layer n are related to those of the preceding layer $(n-1)$ according to the following:

$$\{V^n\}=[K_i^n]\{V^{n-1}\}, \tag{11}$$

with

$$\{V^n\}=\left\{\frac{\partial W}{\partial x},\varphi_x^n,\phi_x^n,\frac{\partial W}{\partial y},\varphi_y^n,\phi_y^n\right\}^{\mathrm{T}}. \tag{12}$$

By applying an iterative process to gradually move from the last layer to the first, a similar equation is established between the last layer n and the first one:

$$\{V^n\}=[K^n]\{V^1\} \tag{13}$$

with

$$[K^n]=\begin{pmatrix} 1 & 0 & 0 & 0 & 0 & 0\\ 0 & \alpha_x^{n-1} & 0 & 0 & \alpha_{xy}^{n-1} & 0\\ \beta_x^{n-1} & \gamma_x^{n-1} & 1 & 0 & \delta_{xy}^{n-1} & 0\\ 0 & 0 & 0 & 1 & 0 & 0\\ 0 & \alpha_{yx}^{n-1} & 0 & 0 & \alpha_y^{n-1} & 0\\ 0 & \delta_{yx}^{n-1} & 0 & \beta_y^{n-1} & \gamma_y^{n-1} & 1 \end{pmatrix}. \tag{14}$$

Eq. (13) takes advantage of this latest equation to allow the displacement field n to be related to layer 1. This displacement field that is therefore a function of the first layer is then used to write the function of Hamilton, which becomes explicitely a function of the first layer only. All this process is a direct result of the transfer matrix equation.

2.4. The multi-layer operator

This operator is established using the variational formulation, which consists in writing a function of energy between two arbitrary times. The function adopted here is that of Hamilton denoted by $\mathscr{H}$ and is constructed in a modular way by superposing the contribution of the multi-layer to that of the boundary condition. $\mathscr{H}$ is given by

$$\mathscr{H}=\int_{t_0}^{t_1}(T-V-V_e)\,\mathrm{d}t, \tag{15}$$

where T and V are, respectively, the kinetic and deformation energies of the multi-layer and V_e is the elastic potential energy of the boundary condition.

2.4.1. Contribution of the multi-layer

For the calculation of T, the density of kinetic energy e_c is first established as

$$e_c = \frac{1}{2}\sum_n \int_{-h_n/2}^{h_n/2} \mu^n \{|\dot{U}^n|^2 + |\dot{V}^n|^2 + |\dot{W}^n|^2\}\, \mathrm{d}(R_n - z). \tag{16}$$

The dot symbol is used to designate the derivative with respect to time, μ^n is the density of each layer; e_c is related to T by

$$T = \int_S e_c \, \mathrm{d}S, \tag{17}$$

S is the area of the structure in the Oxy plane. Eq. (2) allow e_c to be expressed as follows:

$$\begin{aligned} e_c = \frac{1}{2}\Bigg\{ & \delta_1 \left(\frac{\partial^2 W}{\partial x \partial t}\right)^2 + \delta_2 \left(\frac{\partial \varphi_x^1}{\partial t}\right)^2 + \delta_3 \left(\frac{\partial \phi_x^1}{\partial t}\right) + 2\delta_4 \frac{\partial^2 W}{\partial x \partial t}\frac{\partial \varphi_x^1}{\partial t} + 2\delta_5 \frac{\partial^2 W}{\partial x \partial t}\frac{\partial \phi_x^1}{\partial t} + 2\delta_6 \frac{\partial \varphi_x^1}{\partial t}\frac{\partial \phi_x^1}{\partial t} + \delta_7 \left(\frac{\partial^2 W}{\partial y \partial t}\right)^2 \\ & + \delta_8 \left(\frac{\partial \varphi_y^1}{\partial t}\right)^2 + \delta_9 \left(\frac{\partial \phi_y^1}{\partial t}\right)^2 + 2\delta_{10} \frac{\partial^2 W}{\partial y \partial t}\frac{\partial \varphi_y^1}{\partial t} + 2\delta_{11} \frac{\partial^2 W}{\partial y \partial t}\frac{\partial \phi_y^1}{\partial t} + 2\delta_{12} \frac{\partial \varphi_y^1}{\partial t}\frac{\partial \phi_y^1}{\partial t} + \delta_{13} \left(\frac{\partial W}{\partial t}\right)^2 \Bigg\}. \end{aligned} \tag{18}$$

The coefficients δ_i are given in appendix. The density of deformation energy e_d required for the calculation of V is given by

$$e_d = \frac{1}{2}\sum_n \int_{-h_n/2}^{h_n/2} \sigma_{ij}\varepsilon_{ij} d(R_n - z), \tag{19}$$

e_d is related to V by

$$V = \int_S e_d \, \mathrm{d}S, \tag{20}$$

e_d is split into two parts: (i) the first term e_{d1} corresponds to the special case where the orthotropic axes are aligned to coincide with the natural axes of the multi-layer. In this case the ply is assumed to be specially orthotropic. This term is identical in form to the expression proposed in Ref. [13] with respect to simply supported boundary conditions; (ii) the second term denoted e_{d2} results from the generalization of the orthotropic properties and is a consequence of accounting for the terms Q_{16} and Q_{26} in Eq. (4). e_d is written as

$$e_d = e_{d1} + e_{d2} \tag{21}$$

with

$$\begin{aligned} e_{d1} = \frac{1}{2}\sum_n \int_{-h_n/2}^{h_n/2} & \{Q_{11}^n(\varepsilon_{xx}^n)^2 + Q_{22}^n(\varepsilon_{yy}^n)^2 + 2Q_{12}^n\varepsilon_{xx}^n\varepsilon_{yy}^n + 4Q_{66}^n(\varepsilon_{xy}^n)^2 \\ & + 4Q_{44}^n(\varepsilon_{yz}^n)^2 + 4Q_{55}^n(\varepsilon_{xz}^n)^2 + 8Q_{45}^n\varepsilon_{xz}^n\varepsilon_{yz}^n\} d(R_n - z), \end{aligned} \tag{22}$$

$$e_{d2} = \frac{1}{2}\sum_n \int_{-h_n/2}^{h_n/2} \{4Q_{16}^n\varepsilon_{xy}^n\varepsilon_{xx}^n + 4Q_{26}^n\varepsilon_{xy}^n\varepsilon_{yy}^n\} d(R_n - z). \tag{23}$$

After carrying over previously defined expressions, e_{d1} is written as expressed in appendix, while e_{d2} is given by

$$
\begin{aligned}
e_{d2} = \frac{1}{2}\Bigg\{ & \lambda_{39}\left(\frac{\partial^2 W}{\partial x^2}\right)\left(\frac{\partial^2 W}{\partial x \partial y}\right) + \lambda_{40}\left(\frac{\partial^2 W}{\partial x^2}\right)\left(\frac{\partial \varphi_x^1}{\partial y}\right) + \lambda_{41}\left(\frac{\partial^2 W}{\partial x^2}\right)\left(\frac{\partial \phi_x^1}{\partial y}\right) \\
& + \lambda_{42}\left(\frac{\partial^2 W}{\partial x \partial y}\right)\left(\frac{\partial \varphi_x^1}{\partial x}\right) + \lambda_{43}\left(\frac{\partial \varphi_x^1}{\partial x}\right)\left(\frac{\partial \varphi_x^1}{\partial y}\right) + \lambda_{44}\left(\frac{\partial \varphi_x^1}{\partial x}\right)\left(\frac{\partial \phi_x^1}{\partial y}\right) \\
& + \lambda_{45}\left(\frac{\partial^2 W}{\partial x \partial y}\right)\left(\frac{\partial \phi_x^1}{\partial x}\right) + \lambda_{46}\left(\frac{\partial \phi_x^1}{\partial x}\right)\left(\frac{\partial \varphi_x^1}{\partial y}\right) + \lambda_{47}\left(\frac{\partial \phi_x^1}{\partial x}\right)\left(\frac{\partial \phi_x^1}{\partial y}\right) \\
& + \lambda_{48}\left(\frac{\partial^2 W}{\partial x^2}\right)\left(\frac{\partial \varphi_y^1}{\partial x}\right) + \lambda_{49}\left(\frac{\partial^2 W}{\partial x^2}\right)\left(\frac{\partial \phi_y^1}{\partial x}\right) + \lambda_{50}\left(\frac{\partial \varphi_x^1}{\partial x}\right)\left(\frac{\partial \varphi_y^1}{\partial x}\right) \\
& + \lambda_{51}\left(\frac{\partial \varphi_x^1}{\partial x}\right)\left(\frac{\partial \phi_y^1}{\partial x}\right) + \lambda_{52}\left(\frac{\partial \phi_x^1}{\partial x}\right)\left(\frac{\partial \varphi_y^1}{\partial x}\right) + \lambda_{53}\left(\frac{\partial \phi_x^1}{\partial x}\right)\left(\frac{\partial \phi_y^1}{\partial x}\right) \\
& + \lambda_{54}\left(\frac{\partial^2 W}{\partial y^2}\right)\left(\frac{\partial^2 W}{\partial x \partial y}\right) + \lambda_{55}\left(\frac{\partial^2 W}{\partial y^2}\right)\left(\frac{\partial \varphi_x^1}{\partial y}\right) + \lambda_{56}\left(\frac{\partial^2 W}{\partial y^2}\right)\left(\frac{\partial \phi_x^1}{\partial y}\right) \\
& + \lambda_{57}\left(\frac{\partial^2 W}{\partial x \partial y}\right)\left(\frac{\partial \varphi_y^1}{\partial y}\right) + \lambda_{58}\left(\frac{\partial \varphi_y^1}{\partial y}\right)\left(\frac{\partial \varphi_x^1}{\partial y}\right) + \lambda_{59}\left(\frac{\partial \varphi_y^1}{\partial y}\right)\left(\frac{\partial \phi_x^1}{\partial y}\right) \\
& + \lambda_{60}\left(\frac{\partial^2 W}{\partial x \partial y}\right)\left(\frac{\partial \phi_y^1}{\partial y}\right) + \lambda_{61}\left(\frac{\partial \phi_y^1}{\partial y}\right)\left(\frac{\partial \varphi_x^1}{\partial y}\right) + \lambda_{62}\left(\frac{\partial \phi_y^1}{\partial y}\right)\left(\frac{\partial \phi_x^1}{\partial y}\right) \\
& + \lambda_{63}\left(\frac{\partial^2 W}{\partial y^2}\right)\left(\frac{\partial \varphi_y^1}{\partial x}\right) + \lambda_{64}\left(\frac{\partial^2 W}{\partial y^2}\right)\left(\frac{\partial \phi_y^1}{\partial x}\right) + \lambda_{65}\left(\frac{\partial \varphi_y^1}{\partial y}\right)\left(\frac{\partial \varphi_y^1}{\partial x}\right) \\
& + \lambda_{66}\left(\frac{\partial \varphi_y^1}{\partial y}\right)\left(\frac{\partial \phi_y^1}{\partial x}\right) + \lambda_{67}\left(\frac{\partial \phi_y^1}{\partial y}\right)\left(\frac{\partial \varphi_y^1}{\partial x}\right) + \lambda_{68}\left(\frac{\partial \phi_y^1}{\partial y}\right)\left(\frac{\partial \phi_y^1}{\partial x}\right) \\
& + \lambda_{69}\varphi_x^1\varphi_y^1\Bigg\}. \qquad (24)
\end{aligned}
$$

All the parameters λ_i have been calculated and reported in appendix. Eqs. (18), (35) and (24) are reported in Eq. (15) to establish the function of Hamilton.

2.4.2. Contribution of the boundary conditions

The boundary condition modeled in this paper are of elastic type and are expressed by means of different springs. The most important step is the positioning of the different springs, which was determined from minimizing the function of Hamilton in the framework of simply supported boundary conditions. The expressions obtained contain two factors: (i) a first term which represents the natural boundary conditions in terms of stresses; (ii) a second term which expresses the geometrical boundary conditions. By using springs the action is made on the geometrical boundary conditions to force either the translation or the rotation. The interpretation of these special expressions suggests the application of the springs on each of the effects of the first layer, namely on the transverse displacement $W(K_f)$, on the bending rotation $\partial W/\partial s$ (C_f), on the membrane ϕ_s (K_{mx}, K_{my}) and the shear φ_s (K_{sx}, K_{sy}). The equivalent first layer has first to be established and the boundary conditions appear to be expressed by means of a system of six degrees of freedom. The function of Hamilton for the boundary condition is therefore a function of the potential energy which is calculated from the density e_p. Rigidities per unit length are defined so that e_p is expressed as follows:

$$
e_p = \frac{1}{2}\left\{ K_f W^2 + C_f\left(\frac{\partial W}{\partial n}\right)^2 + K_{mx}(\phi_x)^2 + K_{my}(\phi_y)^2 + K_{cx}(\varphi_x)^2 + K_{cy}(\varphi_y)^2 \right\}. \qquad (25)
$$

The Hamilton function of the boundary condition is defined as

$$\mathscr{H}^{bc} = \int_{t_0}^{t_1} \int_{\Gamma} (-e_p)\, \mathrm{d}\Gamma\, \mathrm{d}t, \tag{26}$$

The integral on the contour Γ is split into four in order to account for the individual contributions of the four edges of the plate. This allows the simulation of different boundary conditions on each edge. The account of $\mathscr{H}^{\mathrm{bc}}$ leads to the definition of a stiffness matrix for the boundary condition identical to that defined in Eq. (33). This matrix is also symmetrical with respect to the main diagonal.

2.4.3. Determination of the multi-layer operator

The multi-layer operator is calculated by using the Rayleigh–Ritz method which requires a function basis for the expansion of the different unknowns. A polynomial basis [18] is adopted in order to deal with arbitrary boundary conditions in the contour. This basis is written as

$$\Psi_{nm}(x,y) = \left(\frac{2}{a}x\right)^n \left(\frac{2}{b}y\right)^m, \tag{27}$$

This basis is a mathematical one which has no orthogonality properties. The matrices which are established are full, consequently increasing CPU time. The great advantage is that the parameters required for the calculation of the vibro-acoustic indicators is straightforward using this set of functions. This is the important point which has motivated this choice as will be outlined in a future publication. The different unknowns can therefore be written as

$$\begin{aligned}
W &= \sum_n \sum_m a_{nm} \Psi_n(x) \Psi_m(y);\\
\varphi_x &= \sum_n \sum_m c_{nm} \Psi_n(x) \Psi_m(y);\\
\phi_y &= \sum_n \sum_m d_{nm} \Psi_n(x) \Psi_m(y);\\
\phi_x &= \sum_n \sum_m b_{nm} \Psi_n(x) \Psi_m(y);\\
\varphi_y &= \sum_n \sum_m e_{nm} \Psi_n(x) \Psi_m(y);
\end{aligned} \tag{28}$$

where a_{nm}, b_{nm}, c_{nm}, d_{nm} and e_{nm} are the coefficients of W, ϕ_x, φ_x, ϕ_y and φ_y, respectively, in the basis. After transposing these equations into the Hamilton expression, it is shown that this function is therefore a function of the different coefficients and of their derivatives with respect to time:

$$\mathscr{H} = \int_{t_0}^{t_1} F(\{a_{nm}\}, \{b_{nm}\}, \{c_{nm}\}, \{d_{nm}\}, \{e_{nm}\}\{\dot{a}_{nm}\}, \{\dot{b}_{nm}\}, \{\dot{c}_{nm}\}, \{\dot{d}_{nm}\}, \{\dot{e}_{nm}\})\, \mathrm{d}t. \tag{29}$$

The classical Euler equation is used to minimize $\mathscr{H}$. For the free vibration, this leads to a classical equation of the form

$$-\omega^2 [M_{nmpq}]\{\mathscr{A}_{nm}\} + [K_{nmpq}]\{\mathscr{A}_{nm}\} = \{0\}, \tag{30}$$

where ω is the pulsation. K_{nmpq} includes both the multi-layer and the boundary condition such as

$$K_{nmpq} = K^{\mathrm{m.l.}}_{nmpq} + K^{\mathrm{b.c.}}_{nmpq} \tag{31}$$

and

$$\{A_{nm}\} = \{[a_{nm}], [c_{nm}], [e_{nm}], [b_{nm}], [d_{nm}]\}^{\mathrm{T}}. \tag{32}$$

The global matrices of mass $[M_{nmpq}]$ and stiffness $[K_{nmpq}]$ are matrices of 5×5 blocs. Each bloc is a $N \times N$ matrix. The global matrices are written as follows:

$$M = \begin{bmatrix} [B_1] & [B_2] & [B_3] & [B_4] & [B_5] \\ [B_6] & [B_7] & [B_8] & [B_9] & [B_{10}] \\ [B_{11}] & [B_{12}] & [B_{13}] & [B_{14}] & [B_{15}] \\ [B_{16}] & [B_{17}] & [B_{18}] & [B_{19}] & [B_{20}] \\ [B_{21}] & [B_{22}] & [B_{23}] & [B_{24}] & [B_{25}] \end{bmatrix}. \tag{33}$$

The blocs on the main diagonal represent the pure effects of bending, shear in the x direction, shear in the y direction, membrane in the x direction, membrane in the y direction, respectively. The blocs off the diagonal represent the coupling between the different blocs on the diagonal, which can therefore be investigated separately by setting the appropriate couplings equal to zero.

3. Numerical validation of the model

A numerical code was developed for solving the free vibration. The unknowns were determined by solving a system of linear equations with IMSL mathematical library. All the results presented hereafter have been performed with a number of terms of 10 for the expansion of the unknowns in the series in x and y directions unless otherwise specified. The matrix M and stiffness K have four indices: M_{nmpq} and K_{nmpq}. Each of the indices runs to 10 terms. The validation of the model was established numerically using the material properties listed in Table 1 against data from the literature. The non-dimensional frequencies were used as indicator as calculated from the following equation:

$$\overline{\omega} = \omega \frac{b^2}{h} \left(\frac{\rho}{E_y} \right)^{1/2}, \tag{34}$$

where h is the total thickness of the multi-layer. The convergence of the present formulation has been carefully studied for different cases. Two configurations are reported hereafter, one for a square single-layer composite and a second for a rectangular single-layer composite. The results are presented in Tables 2 and 3, respectively. The convergence is very fast and the frequencies converge to the exact value from values above. The simulations have shown that it is possible to have an adaptative number of terms with regards to the range of frequencies, the low frequencies requiring much less terms for the series to converge. The computation was done with an increasing number of terms in the series from 9 to 15 for the first 20 modes.

The validation was undertaken in three steps: (i) in the single-layer configuration in which the natural frequencies calculated with the present formulation were compared to those obtained using a single-layer model previously published in Ref. [16]. (ii) In a multi-layered configuration in order to validate the multi-layer principle. In this case, a 35 mm structure was split into two, four and ten layers of equal thickness. (iii) Against data available in the literature. Simulations performed using the present model have been done assuming three factors for the transverse shear correction factor, namely 2/3, 5/6 and 1. The aim is to show that the agreement with published data of Ref. [27] depends on the choice of the shear correction factor. Table 4 shows the results for the case of a single-layer composite square plate. The first and third columns are data taken from Ref. [27]. In that paper a formulation using Rayleigh–Ritz method is used along with a set of

Table 1
Material properties of composite plates

Material	E_1 (P_a)	E_2 (P_a)	G_{12} (P_a)	G_{13} (P_a)	G_{23} (P_a)
Material I	6.619×10^8	0.33095×10^8	0.165475×10^8	0.165475×10^8	0.110316667×10^8
		η	ν_{12}	$\frac{\rho}{(\mathrm{kg/m^3})}$	ν_{21}
		0.01	0.25	1000	0.0125

Table 2
Convergence on the natural frequencies for a single-layer square composite

Mode	$N = 9$	$N = 10$	$N = 11$	$N = 12$	$N = 13$
1	0.981	0.981	0.981	0.981	0.981
2	1.392	1.392	1.392	1.392	1.392
3	2.337	2.337	2.336	2.336	2.336
4	3.602	3.602	3.602	3.602	3.602
5	4.420	4.417	4.417	4.417	4.417
6	5.234	5.234	5.234	5.234	5.234
7	5.446	5.446	5.446	5.446	5.446
8	5.949	5.949	5.949	5.949	5.949
9	6.147	6.147	6.146	6.146	6.146
10	6.226	6.225	6.225	6.225	6.225
11	6.550	6.544	6.541	6.541	6.541
12	7.024	7.024	7.024	7.024	7.024
13	7.208	7.208	7.208	7.208	7.208
14	7.539	7.533	7.533	7.532	7.532
15	9.440	9.436	9.436	9.435	9.435
16	9.689	9.681	9.673	9.673	9.672
17	10.380	9.958	9.932	9.914	9.914
18	10.421	10.420	10.420	10.420	10.420
19	10.463	10.463	10.444	10.429	10.428
20	10.548	10.463	10.462	10.462	10.462

Table 3
Convergence on the natural frequencies for a single-layer rectangular composite

Mode	$N = 9$	$N = 10$	$N = 11$	$N = 12$	$N = 13$
1	1.005	1.004	1.004	1.004	1.004
2	2.087	2.087	2.087	2.087	2.087
3	2.827	2.826	2.825	2.825	2.825
4	3.879	3.879	3.879	3.879	3.879
5	4.249	4.249	4.248	4.248	4.248
6	5.410	5.410	5.410	5.410	5.410
7	5.544	5.544	5.542	5.542	5.541
8	5.989	5.985	5.985	5.985	5.985
9	7.979	7.978	7.978	7.978	7.978
10	8.108	8.102	8.100	8.100	8.099
11	8.722	8.722	8.722	8.722	8.722
12	8.980	8.978	8.978	8.977	8.977
13	9.216	9.213	9.213	9.213	9.213
14	9.630	9.630	9.630	9.630	9.630
15	9.818	9.810	9.805	9.805	9.805
16	9.857	9.853	9.851	9.851	9.850
17	10.303	10.294	10.288	10.287	10.287
18	10.536	10.536	10.536	10.536	10.536
19	11.774	11.760	11.760	11.757	11.757
20	11.903	11.892	11.882	11.882	11.882

orthogonal polynomial functions for the basis [30]. In that study the simulations were done for transversely isotropic materials. Two models were used and are referenced as models I and II. The former is based on the three-dimensional elasticity theory while the latter does not account for Young modulus in the z direction E_z and the Poisson ratios v_{xz} and v_{yz}. The results of the present formulation are presented in column 4. By comparing both set of data it is shown that the agreement greatly depends on the value of the shear correction factor. This point is not well established in the literature, the value generally adopted depends on the material

Table 4
First non-dimensional natural frequencies for a single-layer composite square plate—number of terms in the expansion of the series: 10—shear correction factor (sfc) varying

Mode	Model I (Hz) Ref. [27]	Model II (Hz) Ref. [27]	Present model (Hz) (scf = 2/3)	Present model (Hz) (scf = 5/6)	Present model (Hz) (scf = 1)
1	0.98	0.98	0.97	0.98	0.99
2	1.39	1.39	1.39	1.39	1.40
3	2.34	2.34	2.31	2.34	2.36
4	3.61	3.60	3.55	3.60	3.63
5	4.43	4.42	4.34	4.42	4.48
6	5.25	5.25	5.24	5.23	5.38
7	5.46	5.46	5.91	5.45	5.60
8	6.17	6.16	6.23	6.15	6.22
9	6.58	6.54	6.39	6.54	6.66
10	7.24	7.20	7.25	7.20	7.34

Table 5
First non-dimensional natural frequencies for an angle-ply composite square multi-layered plate: $[30, -30, -30, 30]$—number of terms in the expansion of the series: 10—(*) Frequency missing—shear correction factor (sfc) varying

Mode	Model I (Hz) Ref. [27]	Model II (Hz) Ref. [27]	Present model (Hz) (scf = 2/3)	Present model (Hz) (scf = 5/6)	Present model (Hz) (scf = 1)
1	1.47	1.47	1.47	1.47	1.47
2	1.78	1.79	1.77	1.79	1.81
3	3.56	3.57	3.51	3.60	3.67
4	3.81	3.82	3.75	3.83	3.88
5	4.03	4.04	3.93	4.05	4.15
6	5.52	5.53	5.33	5.56	5.73
7	5.86	5.85	5.67	5.88	6.05
8	6.59	6.63	6.45	6.65	6.91
9	7.90	7.92	7.81	7.97	8.29
10	8.12	8.10	(*)	8.15	8.41

Table 6
First natural frequencies for an angle-ply composite square multi-layered plate: $[45, -45, -45, 45]$—number of terms in the expansion of the series: 10—(*) frequency missing—shear correction factor (sfc) varying

Mode	Model I (Hz) Ref. [27]	Model II (Hz) Ref. [27]	Present model (Hz) (scf = 2/3)	Present model (Hz) (scf = 5/6)	Present model (Hz) (scf = 1)
1	1.55	1.55	1.54	1.55	1.55
2	1.89	1.89	1.87	1.90	1.92
3	3.71	3.70	3.60	3.72	3.80
4	3.80	3.81	3.73	3.85	3.93
5	4.00	4.01	3.90	4.02	4.10
6	6.14	6.16	5.95	6.20	6.39
7	6.17	6.18	5.98	6.23	6.41
8	6.58	6.60	6.60	6.69	6.89
9	7.93	6.94	7.02	6.97	7.02
10	8.77	8.78	(*)	8.84	9.25

and could vary with the type of lay-up. Two cases of angle-ply composites are presented in Tables 5 and 6 for four layers with the sequence of $[30, -30, -30, 30]$ and $[45, -45, -45, 45]$, respectively. The agreement is very good between both simulation. The same exercise of validation was performed on a rectangular composite plate for single-layer, angle-ply $[30, -30, -30, 30]$. The same level of agreement is established. At this point it

must be noticed that a shear correction factor is accounted for the non-parabolic distribution of the shear stresses. The value adopted in the present formulation has been arbitrarily fixed to a constant value but nothing guarantees that this should be constant through the layers and that the factor should be the same for different multi-layers with different properties (Tables 7 and 8).

4. Sensitivity on the stiffness at the boundaries

In this section a sensitivity analysis done on varying the stiffness of the boundary conditions on simply supported boundary condition is presented. Basically to realize a simply supported boundary condition the displacement must be blocked by taking a high value of the stiffness. Investigation has been performed by varying the stiffness from high to low between $K = 10^{16}\,\mathrm{N/m}$ and $K = 10^{5}\,\mathrm{N/m}$. These stiffnesses are expressed as dimensional values. Seven configurations have therefore been simulated. The dimensional natural frequencies are presented in Table 9. All these simulations are performed using ten (10) terms in the series. The results obtained for $K = 10^{14}\,\mathrm{N/m}$ are the typical values obtained by the ideal case to properly model the simply-supported boundary condition stiffness required at the boundaries. This statement is drawn from further analysis done on forced vibration (not presented in the present paper) and comparison with analytical approach for simply supported boundary condition. Table 9 highlights that the choice of the stiffness at the boundaries is very critical for successfully computing the natural frequencies. On one hand, if the stiffness is

Table 7
First natural frequencies for a single-layer composite rectangular plate—number of terms in the expansion of the series: 10—(*) frequency missing—shear correction factor (sfc) varying

Mode	Model I (Hz) Ref. [27]	Model II (Hz) Ref. [27]	Present model (Hz) (scf = 2/3)	Present model (Hz) (scf = 5/6)	Present model (Hz) (scf = 1)
1	1.45	1.45	1.44	1.45	1.46
2	3.01	3.00	2.99	3.01	3.03
3	3.98	3.97	3.92	3.98	4.03
4	5.25	5.25	5.04	5.24	5.38
5	5.70	5.70	5.47	5.69	5.85
6	7.33	7.31	7.02	7.30	7.50
7	7.40	7.36	7.20	7.37	7.51
8	8.10	8.06	7.99	8.07	8.22
9	10.50	10.49	(*)	10.48	10.55
10	10.54	10.53	(*)	10.55	10.78

Table 8
First natural frequencies for an angle-ply composite rectangular stratified plate: $[30, -30, -30, 30]$—number of terms in the expansion of the series: 10—(*) frequency missing—shear correction factor (sfc) varying

Mode	Model I (Hz) Ref. [27]	Model II (Hz) Ref. [27]	Present model (Hz) (scf = 2/3)	Present model (Hz) (scf = 5/6)	Present model (Hz) (scf = 1)
1	2.31	2.32	2.31	2.34	2.36
2	2.87	2.87	2.84	2.88	2.91
3	4.91	4.92	4.76	4.94	5.07
4	5.04	5.07	4.98	5.14	5.26
5	5.65	5.66	5.46	5.68	5.84
6	8.16	8.23	8.00	8.38	8.67
7	8.41	8.42	8.02	8.48	8.81
8	9.13	9.12	8.76	9.17	9.48
9	9.26	9.25	8.84	9.29	9.66
10	11.12	11.14	10.48	11.20	11.79

Table 9
Sensitivity on the stiffness at the boundaries—dimensional natural frequencies for simply supported BC—the values labeled with an asterix are not the natural frequencies but rather the results due to ill-conditioned matrices—number of terms in the expansion of the series: 10

1	25.49 (*)	96.83	96.79	78.73	36.91 (*)	3.80 (*)
2	44.83 (*)	137.2	137.13	96.56 (*)	37.31 (*)	3.80 (*)
3	66.31 (*)	183.77 (*)	183.51 (*)	101.11 (*)	41.01	5.35
4	121.74 (*)	183.77 (*)	183.51 (*)	115.06	65.07 (*)	6.59 (*)
5	136.18 (*)	218.6	218.5	174.72	66.12	7.56 (*)
6	162.27 (*)	266.51	266.36	184.41	69.99	7.56 (*)
7	183.77 (*)	287.87	287.67	184.79 (*)	91.31	37.36
8	183.77 (*)	315.49 (*)	315.3 (*)	195.76	98.59	52.16
9	206.33 (*)	327.9	327.78	244.77	127.8	86.96
10	210.13 (*)	338.79	338.54	260.8 (*)	157.55	133.50

too high to constraint the displacement ($K = 10^{16}\,\mathrm{N/m}$) the matrices are ill-conditioned resulting in incapability in calculating the eigenvalues. On the other hand, if the stiffness is too low (for example $K = 10^{5}\,\mathrm{N/m}$) the motion is not blocked. However, a low stiffness value could be a way of simulating soft boundary conditions. A theoretical investigation is presently under way regarding this point. In Table 9, the values labeled with an asterisk are not the accurate natural frequencies but rather the results due to ill-conditioned matrices.

5. Conclusions

The work reported in this paper was aimed at developing a new modeling tool to compute the natural frequencies of advanced multi-layered composites. Although the general formulation developed by the author includes arbitrary elastic boundary conditions through artificial springs, the present paper addresses the case of free–free boundary conditions. The operator of the multi-layer has been established using Rayleigh–Ritz method along with a non-orthogonal polynomial basis available in the literature. The multi-layer is of hybrid type, which combines the advantages of the first-order shear deformation theory and a pure multi-layered modeling. The displacement field is defined for each layer and includes the bending and in-plane motions, i.e. stretching and shearing. This results in five unknowns in the framework of a two-dimensional modeling. For each layer anisotropic properties are accounted for through general orthotropy. The originality of the present approach is (1) the modeling of anisotropic properties for each layer; (2) the application of the transfer matrix formulation of Ref. [12] to layers made of more advanced general orthotropic materials; (3) the modeling of arbitray boundary conditions through artificial springs to control the translational and rotational motions of each wave. The transfer matrix is defined from appropriate interface conditions between two adjacent layers, which allows (i) the parameters of the last layer to be iteratively related to those of the first layer and (ii) to keep the number of unknowns constant to five independently of the number of the layers involved. The model was then validated step by step. First the model was validated numerically in a single-layer isotropic configuration against results predicted using a model previously developed by the author [34,35]. Then the multi-layer principle was investigated by splitting a single-layer into two, four and ten layers. Finally, comparison was done between simulations with the proposed model against existing data in the literature for one layer and four-layered angle-ply composites. Simulations done with the proposed model have been done with three values of shear correction factor required in the first-shear deformation theory. Comparison with available data in the literature suggests that more investigation should be done to establish the typical values of shear correction factors in the case of stratified materials. In all cases shown in the present study a very good agreement was observed assessing the validity of the proposed modeling. Further work is under investigation to extend the validation to different types of boundary conditions and to the case of forced vibration for the general case of vibro-acoustics. As stated in the introduction, the ultimate goal is the development of an efficient component-level predictive tool to be interfaced with an optimizer for design purposes at an early stage of development cycle.

Acknowledgments

The author expresses his thanks to all the reviewers who provided critical comments and valuable suggestions.

Appendix A. Definition of coefficients δ_i

$$
\begin{aligned}
\delta_1 &= \sum_n \left[\mu^n h_n (\beta_x^{(n-1)})^2 + \mu^n \frac{h_n^3}{12}\right],\\
\delta_2 &= \sum_n \left[\mu^n h_n (\gamma_x^{(n-1)})^2 + \mu^n \frac{h_n^3}{12}(\alpha_x^{(n-1)})^2\right],\\
\delta_3 &= \sum_n \mu^n h_n,\\
\delta_4 &= \sum_n \left[\mu^n h_n \beta_x^{(n-1)}\gamma_x^{(n-1)} + \mu^n \frac{h_n^3}{12}(\alpha_x^{(n-1)})\right],\\
\delta_5 &= \sum_n \mu^n h_n \beta_x^{(n-1)},\\
\delta_6 &= \sum_n \mu^n h_n \gamma_x^{(n-1)},\\
\delta_7 &= \sum_n \left[\mu^n h_n (\beta_y^{(n-1)})^2 + \mu^n \frac{h_n^3}{12}\right],\\
\delta_8 &= \sum_n \left[\mu^n h_n (\gamma_y^{(n-1)})^2 + \mu^n \frac{h_n^3}{12}(\alpha_y^{(n-1)})^2\right],\\
\delta_9 &= \delta_3,\\
\delta_{10} &= \sum_n \left[\mu^n h_n \beta_y^{(n-1)}\gamma_y^{(n-1)} + \mu^n \frac{h_n^3}{12}(\alpha_y^{(n-1)})\right],\\
\delta_{11} &= \sum_n \mu^n h_n \beta_y^{(n-1)},\\
\delta_{12} &= \sum_n \mu^n h_n \gamma_y^{(n-1)},\\
\delta_{13} &= \delta_3.
\end{aligned}
$$

Appendix B. Expression of e_{d1}

$$
\begin{aligned}
e_{d1} = \frac{1}{2}\Bigg\{ & \lambda_1\left(\frac{\partial^2 W}{\partial x^2}\right)^2 + \lambda_2\left(\frac{\partial \varphi_x^1}{\partial x}\right)^2 + \lambda_3\left(\frac{\partial \phi_x^1}{\partial x}\right)^2 + \lambda_4\left(\frac{\partial^2 W}{\partial x^2}\right)\left(\frac{\partial \varphi_x^1}{\partial x}\right)\\
& + \lambda_5\left(\frac{\partial^2 W}{\partial x^2}\right)\left(\frac{\partial \phi_x^1}{\partial x}\right) + \lambda_6\left(\frac{\partial \varphi_x^1}{\partial x}\right)\left(\frac{\partial \phi_x^1}{\partial x}\right) + \lambda_7\left(\frac{\partial^2 W}{\partial y^2}\right)^2\\
& + \lambda_8\left(\frac{\partial \varphi_y^1}{\partial y}\right)^2 + \lambda_9\left(\frac{\partial \phi_y^1}{\partial y}\right)^2 + \lambda_{10}\left(\frac{\partial^2 W}{\partial y^2}\right)\left(\frac{\partial \varphi_y^1}{\partial y}\right)\\
& + \lambda_{11}\left(\frac{\partial^2 W}{\partial y^2}\right)\left(\frac{\partial \phi_y^1}{\partial y}\right) + \lambda_{12}\left(\frac{\partial \varphi_y^1}{\partial y}\right)\left(\frac{\partial \phi_y^1}{\partial y}\right)
\end{aligned}
$$

$$
\begin{aligned}
&+\lambda_{13}\left(\frac{\partial^2 W}{\partial x^2}\right)\left(\frac{\partial^2 W}{\partial y^2}\right)+\lambda_{14}\left(\frac{\partial^2 W}{\partial x^2}\right)\left(\frac{\partial \varphi_y^1}{\partial y}\right)+\lambda_{15}\left(\frac{\partial^2 W}{\partial x^2}\right)\left(\frac{\partial \phi_y^1}{\partial y}\right)\\
&+\lambda_{16}\left(\frac{\partial^2 W}{\partial y^2}\right)\left(\frac{\partial \varphi_x^1}{\partial x}\right)+\lambda_{17}\left(\frac{\varphi_x^1}{\partial x}\right)\left(\frac{\partial \varphi_y^1}{\partial \varphi_y^1}\right)+\lambda_{18}\left(\frac{\varphi_x^1}{\partial x}\right)\left(\frac{\partial \phi_y^1}{\partial y}\right)\\
&+\lambda_{19}\left(\frac{\partial^2 W}{\partial y^2}\right)\left(\frac{\partial \phi_x^1}{\partial x}\right)+\lambda_{20}\left(\frac{\partial \phi_x^1}{\partial \varphi_y^1}\right)\left(\frac{\partial \varphi_y^1}{\partial y}\right)+\lambda_{21}\left(\frac{\partial \phi_x^1}{\partial x}\right)\left(\frac{\partial \phi_y^1}{\partial y}\right)\\
&+\lambda_{22}\left(\frac{\partial^2 W}{\partial x\partial y}\right)^2+\lambda_{23}\left(\frac{\partial \varphi_x^1}{\partial y}\right)^2+\lambda_{24}\left(\frac{\partial \varphi_y^1}{\partial x}\right)^2+\lambda_{25}\left(\frac{\partial \phi_x^1}{\partial y}\right)^2\\
&+\lambda_{26}\left(\frac{\partial \phi_y^1}{\partial x}\right)^2+\lambda_{27}\left(\frac{\partial^2 W}{\partial x\partial y}\right)\left(\frac{\partial \varphi_x^1}{\partial y}\right)+\lambda_{28}\left(\frac{\partial^2 W}{\partial x\partial y}\right)\left(\frac{\partial \varphi_y^1}{\partial x}\right)\\
&+\lambda_{29}\left(\frac{\partial^2 W}{\partial x\partial y}\right)\left(\frac{\partial \phi_x^1}{\partial y}\right)+\lambda_{30}\left(\frac{\partial^2 W}{\partial x\partial y}\right)\left(\frac{\partial \phi_y^1}{\partial x}\right)+\lambda_{31}\left(\frac{\varphi_x^1}{\partial y}\right)\left(\frac{\partial \varphi_y^1}{\partial x}\right)\\
&+\lambda_{32}\left(\frac{\partial \varphi_x^1}{\partial y}\right)\left(\frac{\partial \phi_x^1}{\partial y}\right)+\lambda_{33}\left(\frac{\partial \varphi_x^1}{\partial y}\right)\left(\frac{\partial \phi_y^1}{\partial x}\right)+\lambda_{34}\left(\frac{\partial \phi_x^1}{\partial y}\right)\left(\frac{\partial \varphi_y^1}{\partial x}\right)\\
&+\lambda_{35}\left(\frac{\partial \phi_y^1}{\partial x}\right)\left(\frac{\partial \varphi_y^1}{\partial x}\right)+\lambda_{36}\left(\frac{\partial \phi_x^1}{\partial y}\right)\left(\frac{\partial \phi_y^1}{\partial x}\right)+\lambda_{37}(\varphi_x^1)^2+\lambda_{38}(\varphi_y^1)^2\Bigg\}.
\end{aligned}
$$

Appendix C. Definition of coefficients λ_i—contribution of special orthotropy

$$
\begin{aligned}
\lambda_1 &= \sum_n Q_{11}^n\left(h_n(\beta_x^{(n-1)})^2+\frac{h_n^3}{12}\right),\\
\lambda_2 &= \sum_n Q_{11}^n\left(h_n(\gamma_x^{(n-1)})^2+\frac{h_n^3}{12}(\alpha_x^{(n-1)})^2\right),\\
\lambda_3 &= \sum_n Q_{11}^n h_n,\\
\lambda_4 &= \sum_n 2Q_{11}^n\left(h_n\beta_x^{(n-1)}\gamma_x^{(n-1)}+\frac{h_n^3}{12}\alpha_x^{(n-1)}\right),\\
\lambda_5 &= \sum_n 2Q_{11}^n(h_n\beta_x^{(n-1)}),\\
\lambda_6 &= \sum_n 2Q_{11}^n(h_n\gamma_x^{(n-1)}),\\
\lambda_7 &= \sum_n Q_{22}^n\left(h_n(\beta_y^{(n-1)})^2+\frac{h_n^3}{12}\right),\\
\lambda_8 &= \sum_n Q_{22}^n\left(h_n(\gamma_y^{(n-1)})^2+\frac{h_n^3}{12}(\alpha_y^{(n-1)})^2\right),\\
\lambda_9 &= \sum_n Q_{22}^n h_n,\\
\lambda_{10} &= \sum_n 2Q_{22}^n\left(h_n\beta_y^{(n-1)}\gamma_y^{(n-1)}+\frac{h_n^3}{12}\alpha_y^{(n-1)}\right),
\end{aligned}
$$

$$\lambda_{11} = \sum_n 2Q_{22}^n(h_n\beta_y^{(n-1)}),$$

$$\lambda_{12} = \sum_n 2Q_{22}^n(h_n\gamma_y^{(n-1)}),$$

$$\lambda_{13} = \sum_n 2Q_{12}^n\left(h_n\beta_x^{(n-1)}\beta_y^{(n-1)} + \frac{h_n^3}{12}\right),$$

$$\lambda_{14} = \sum_n 2Q_{12}^n\left(h_n\beta_x^{(n-1)}\gamma_y^{(n-1)} + \frac{h_n^3}{12}\alpha_y^{(n-1)}\right),$$

$$\lambda_{15} = \sum_n 2Q_{12}^n(h_n\beta_x^{(n-1)}),$$

$$\lambda_{16} = \sum_n 2Q_{12}^n\left(h_n\beta_y^{(n-1)}\gamma_x^{(n-1)} + \frac{h_n^3}{12}\alpha_x^{(n-1)}\right),$$

$$\lambda_{17} = \sum_n 2Q_{12}^n\left(h_n\gamma_x^{(n-1)}\gamma_y^{(n-1)} + \frac{h_n^3}{12}\alpha_x^{(n-1)}\alpha_y^{(n-1)}\right),$$

$$\lambda_{18} = \sum_n 2Q_{12}^n\left(\frac{h_n^3}{12}\gamma_x^{(n-1)}\right),$$

$$\lambda_{19} = \sum_n 2Q_{12}^n(h_n\beta_y^{(n-1)}),$$

$$\lambda_{20} = \sum_n 2Q_{12}^n(h_n\gamma_y^{(n-1)}),$$

$$\lambda_{21} = \sum_n 2Q_{12}^n h_n,$$

$$\lambda_{22} = \sum_n Q_{66}^n\left(h_n(\beta_x^{(n-1)} + \beta_y^{(n-1)})^2 + 4\frac{h_n^3}{12}\right)^2,$$

$$\lambda_{23} = \sum_n Q_{66}^n\left(h_n(\gamma_x^{(n-1)})^2 + \frac{h_n^3}{12}(\alpha_x^{(n-1)})^2\right),$$

$$\lambda_{24} = \sum_n Q_{66}^n\left(h_n(\gamma_y^{(n-1)})^2 + \frac{h_n^3}{12}(\alpha_y^{(n-1)})^2\right),$$

$$\lambda_{25} = \sum_n Q_{66}^n h_n,$$

$$\lambda_{26} = \lambda_{25},$$

$$\lambda_{27} = \sum_n 2Q_{66}^n\left(h_n\beta_x^{(n-1)}\gamma_x^{(n-1)} + h_n\beta_y^{(n-1)}\gamma_x^{(n-1)} + 2\frac{h_n^3}{12}\alpha_x^{(n-1)}\right),$$

$$\lambda_{28} = \sum_n 2Q_{66}^n\left(h_n\beta_y^{(n-1)}\gamma_y^{(n-1)} + h_n\beta_x^{(n-1)}\gamma_y^{(n-1)} + 2\frac{h_n^3}{12}\alpha_y^{(n-1)}\right),$$

$$\lambda_{29} = \sum_n 2Q_{66}^n(h_n\beta_x^{(n-1)} + h_n\beta_y^{(n-1)}),$$

$$\lambda_{30} = \sum_n 2Q_{66}^n(h_n\beta_y^{(n-1)} + h_n\beta_x^{(n-1)}),$$

$$\lambda_{31} = \sum_n 2Q_{66}^n\left(h_n\gamma_x^{(n-1)}\gamma_y^{(n-1)} + \frac{h_n^3}{12}\alpha_x^{(n-1)}\alpha_y^{(n-1)}\right),$$

$$\lambda_{32} = \sum_n 2Q_{66}^n(h_n\gamma_x^{(n-1)}),$$

$$\lambda_{33} = \lambda_{32},$$
$$\lambda_{34} = \sum_n 2Q_{66}^n (h_n \gamma_y^{(n-1)}),$$
$$\lambda_{35} = \lambda_{34},$$
$$\lambda_{36} = \sum_n 2Q_{66}^n h_n,$$
$$\lambda_{37} = \sum_n Q_{55}^n (h_n (\alpha_x^{(n-1)})^2),$$
$$\lambda_{38} = \sum_n Q_{44}^n (h_n (\alpha_y^{(n-1)})^2).$$

Appendix D. Definition of coefficients λ_i—contribution of generalized orthotropy

$$\lambda_{39} = \sum_n 2Q_{16}^n \left(h_n (\beta_x^{(n-1)})^2 + h_n \beta_x^{(n-1)} \beta_y^{n-1} + 2\frac{h_n^3}{12} \right),$$
$$\lambda_{40} = \sum_n 2Q_{16}^n \left(h_n (\beta_x^{(n-1)})(\gamma_x^{(n-1)}) + \frac{h_n^3}{12} \alpha_x^{(n-1)} \right),$$
$$\lambda_{41} = \sum_n 2Q_{16}^n (h_n (\beta_x^{(n-1)})),$$
$$\lambda_{42} = \sum_n 2Q_{16}^n \left(h_n \beta_x^{(n-1)} \gamma_x^{(n-1)} + 2\frac{h_n^3}{12} \alpha_x^{(n-1)} + h_n \beta_y^{(n-1)} \gamma_x^{n-1} \right),$$
$$\lambda_{43} = \sum_n 2Q_{16}^n \left(h_n (\gamma_x^{(n-1)})^2 + \frac{h_n^3}{12} (\alpha_x^{(n-1)})^2 \right),$$
$$\lambda_{44} = \sum_n 2Q_{16}^n (h_n \gamma_x^{(n-1)}),$$
$$\lambda_{45} = \sum_n 2Q_{16}^n (h_n \beta_x^{(n-1)} + h_n \beta_y^{(n-1)}),$$
$$\lambda_{46} = \sum_n 2Q_{16}^n (h_n \gamma_x^{(n-1)}),$$
$$\lambda_{47} = \sum_n 2Q_{16}^n h_n,$$
$$\lambda_{48} = \sum_n 2Q_{16}^n \left(h_n \beta_x^{(n-1)} \gamma_y^{n-1} + \frac{h_n^3}{12} \alpha_y^{(n-1)} \right),$$
$$\lambda_{49} = \sum_n 2Q_{16}^n h_n \beta_x^{(n-1)},$$
$$\lambda_{50} = \sum_n 2Q_{16}^n \left(h_n \gamma_x^{(n-1)} \gamma_y^{(n-1)} + \frac{h_n^3}{12} \alpha_x^{(n-1)} \alpha_y^{(n-1)} \right),$$
$$\lambda_{51} = \lambda_{46},$$
$$\lambda_{52} = \sum_n 2Q_{16} h_n \gamma_y^{n-1},$$
$$\lambda_{53} = \lambda_{47},$$
$$\lambda_{54} = \sum_n 2Q_{26}^n \left(h_n \beta_x^{(n-1)} \beta_y^{(n-1)} + h_n (\beta_y^{(n-1)})^2 + 2\frac{h_n^3}{12} \right),$$

$$\lambda_{55} = \sum_n 2Q_{26}^n \left(h_n \beta_y^{(n-1)} \gamma_x^{(n-1)} + \frac{h_n^3}{12} \alpha_x^{(n-1)} \right),$$

$$\lambda_{56} = \sum_n 2Q_{26}^n h_n \beta_y^{n-1},$$

$$\lambda_{57} = \sum_n 2Q_{26}^n \left(h_n \beta_x^{(n-1)} \gamma_y^{(n-1)} + h_n \beta_y^{(n-1)} \gamma_y^{(n-1)} + \frac{h_n^3}{12} 2\alpha_y^{(n-1)} \right),$$

$$\lambda_{58} = \sum_n 2Q_{26}^n \left(h_n \gamma_x^{(n-1)} \gamma_y^{(n-1)} + \frac{h_n^3}{12} \alpha_x^{(n-1)} \alpha_y^{(n-1)} \right),$$

$$\lambda_{59} = \sum_n 2Q_{26}^n h_n \gamma_y^{(n-1)},$$

$$\lambda_{60} = \sum_n 2Q_{26}^n (h_n \beta_x^{(n-1)} + h_n \beta_y^{(n-1)}),$$

$$\lambda_{61} = \sum_n 2Q_{26}^n h_n \gamma_x^{(n-1)},$$

$$\lambda_{62} = \sum_n 2Q_{26}^n h_n,$$

$$\lambda_{63} = \sum_n 2Q_{26}^n \left(h_n \beta_y \gamma_y^{(n-1)} + \frac{h_n^3}{12} \alpha_y^{(n-1)} \right),$$

$$\lambda_{64} = \lambda_{56},$$

$$\lambda_{65} = \sum_n 2Q_{26}^n \left(h_n (\gamma_y^{(n-1)})^2 + \frac{h_n^3}{12} (\alpha_y^{(n-1)})^2 \right),$$

$$\lambda_{66} = \lambda_{59},$$

$$\lambda_{67} = \lambda_{59},$$

$$\lambda_{68} = \lambda_{62},$$

$$\lambda_{69} = \sum_n 2Q_{45}^n h_n \alpha_x^{(n-1)} \alpha_y^{(n-1)}.$$

References

[1] A.K. Noor, Mechanics of anisotropic plates and shells—a new look at an old subject, *Computers and Structures* 44 (3) (1992) 499–514.
[2] R.M. Jones, *Mechanics of Composite Materials*, Taylor & Francis Inc., Philadelphia, 1999.
[3] J.N. Reddy, *Mechanics of Laminated Composite Plates—Theory and Analysis*, CRC Press, New York, 1997.
[4] R.D. Mindlin, Influence of rotatory inertia and shear on flexural motions of isotropic elastic plates, *ASME Journal of Applied Mechanics* 18 (A31) (1951).
[5] J.N. Reddy, A generalization of two-dimensional theory of laminated composite plate, *Communications in Applied Numerical Methods* 3 (1987) 173–180.
[6] X. Lu, D. Liu, Interlayer shear slip theory for cross-ply laminates with nonrigid interfaces, *AIAA Journal* 30 (4) (1992) 1063–1073.
[7] C. Sun, J.M. Whitney, Theories for the dynamic response of laminated plates, *AIAA Journal* 11 (2) (1973) 178–183.
[8] R.D. Ford, P. Lord, A.W. Walker, Sound transmission through sandwich constructions, *Journal of Sound and Vibration* 5 (1) (1967) 9–21.
[9] C.P. Smolenski, E.M. Krokosky, Dilatational-mode sound transmission in sandwich panels, *Journal of the Acoustical Society of America* 54 (6) (1973) 1449–1457.
[10] J.A. Moore, R.H. Lyon, Sound transmission loss characteristics of sandwich panel constructions, *Journal of the Acoustical Society of America* 89 (2) (1991) 777–791.
[11] S. Narayanan, R.L. Shanbag, Sound transmission through a damped sandwich panel, *Journal of Sound and Vibration* 80 (3) (1982) 315–327.
[12] J.L. Guyader, C. Lesueur, Acoustics transmission through orthotropic multilayered plates, part I: plate vibration modes, *Journal of Sound and Vibration* 58 (1) (1978) 51–68.
[13] J.L. Guyader, C. Lesueur, Acoustic transmission through orthotropic multilayered plates, part II: transmission loss, *Journal of Sound and Vibration* 58 (1) (1978) 69–86.
[14] C.Y. Lee, D. Liu, Layer reduction technique for composite laminate analysis, *Computers and Structures* 44 (6) (1992) 1305–1315.

[15] S. Narayanan, R.L. Shanbag, Sound transmission through elastically supported sandwich panels into a rectangular enclosure, *Journal of Sound and Vibration* 77 (2) (1981) 251–270.
[16] R. Woodcock, J. Nicolas, A generalized model for predicting the sound transmission properties of orthotropic plates with general boundary conditions, *Journal of the Acoustical Society of America* 97 (2) (1995) 1099–1112.
[17] R. Woodcock, Modeling of Sound Transmission of Single-layer and Multi-layered Anisotropic Composite Structures with Arbitrary Boundary Conditions, PhD Thesis in French, Sherbrooke University, Québec, Canada, 1993.
[18] A. Berry, Vibration and Acoustic Radiation of Complex Plane Structures Embedded in a Light or Heavy Fluid, PhD Thesis in French, Sherbrooke University, Québec, Canada, 1991.
[27] P.S. Frederiksen, Single-layer plate theories applied to the flexural vibration of completely free thick laminates, *Journal of Sound and Vibration* 186 (5) (1995) 743–759.
[28] M. Amabili, R. Garziera, A technique for the systematic choice of admissible functions in the Rayleigh–Ritz method, *Journal of Sound and Vibration* 224 (3) (1999) 519–539.
[29] D.J. Gorman, Free in-plane vibration analysis of rectangular plates by the method of superposition, *Journal of Sound and Vibration* 272 (2004) 831–851.
[30] R.B. Bhat, Natural frequencies of rectangular plates using characteristic orthogonal polynomials in Rayleigh–Ritz method, *Journal of Sound and Vibration* 102 (4) (1985) 493–499.
[31] A. Berry, J.-L. Guyader, J. Nicolas, A general formulation for the sound radiation from rectangular baffled plates with arbitrary boundary conditions, *Journal of the Acoustical Society of America* 88 (6) (1990) 2792–2802.
[32] S. Chakraverty, R.B. Bhat, I. Stiharu, Recent research on vibration of structures using boundary characteristic orthogonal polynomials in the Rayleigh–Ritz method, *The Shock and Vibration Digest* 31 (3) (1999) 187–194.
[33] R.B. Bhat, Nature of stationarity of the natural frequencies at the natural modes in the Rayleigh–Ritz method, *Journal of Sound and Vibration* 203 (2) (1997) 251–263.
[34] R. Woodcock, G. Ebbitt, Modeling the vibro-acoustical behavior of multi-layered composite systems, *SAE Noise & Vibration Conference. Paper 2001-01-1413*, Traverse City, Michigan, May 2001.
[35] R.L. Woodcock, R.B. Bhat, I.G. Stiharu, Effect of ply orientation on the in-plane vibration of single-layer composite plates, *Journal of Sound and Vibration* (2007), doi:10.1016/j.jsv.2007.10.028.